A 2-D finite element model for wave propagation into arbitrary inhomogeneous materials

E. Sumbar, F.S. Chute, and F.E. Vermeulen

Applied Electromagnetics Laboratory
Department of Electrical Engineering
University of Alberta
Edmonton, Alberta, Canada T6G 2G7
(403) 492-3332

Abstract

A finite element program called FEAST, coded in FORTRAN, provides a frequency domain (sinusoidal steady state) solution to Maxwell's equations in cylindrical coordinates. By imposing a radiation or impedance boundary condition at the far boundary of the finite element mesh, FEAST models the near fields of axially symmetric antennas in arbitrary inhomogeneous materials. The program has been validated by reproducing the driving point impedances and current distributions of several antenna configurations for which theoretical and experimental results are available in the published literature.

Introduction

Two numerical approaches for modelling the electromagnetic radiation from isolated wire antennas are the moment method (MoM) (Harrington 1968) and the related technique of boundary integral elements (BEM or BIE) (Brebbia 1984). The application of either of these procedures to the study of bare antennas operating in an infinite homogeneous environment is straightforward. To analyze radiating systems that are inhomogeneous — an antenna with a dielectric coating, for example — a method is employed whereby the infinite problem domain is divided into two distinct regions (McDougall and Webb 1989; Morgan *et al.* 1977; McDonald and Wexler 1972). Accordingly, an artificial boundary is erected so as to collect all of the inhomogeneities associated with the problem into the boundary's interior zone, leaving the infinite exterior region homogeneous. A solution to the interior problem may be subsequently formulated with an appropriate bounded method such as finite elements; the exterior problem, meanwhile, may be handled with one of the techniques mentioned above. Satisfying appropriate boundary conditions at the interface between the two regions couples the two expressions and permits a solution to be calculated (for example, Paulsen *et al.* 1988).

In this paper, we introduce an alternative method for solving the near-field antenna radiation problem which avoids the com-

plication of coupling a bounded-problem description to an unbounded-problem description. Using finite elements, the technique is applicable to azimuthally symmetric antennas propagating into inhomogeneous lossy dielectrics. And rather than use infinite elements to model the far-field region, we have adopted radiation boundary conditions.

A relatively compact implementation of the method has been developed for use on Macintosh II personal computers. The program comprises approximately 5000 lines of FORTRAN and will be referred to as FEAST. It yields a full field description throughout the domain of the problem from which the driving point admittance and current distribution along the antenna can be easily derived.

The following sections outline the finite element approach implemented by FEAST for the solution of antenna–radiation problems. In addition, the validity of the method is demonstrated in a comparison between certain published antenna characteristics and the results obtained with FEAST.

Theory

Consider the antenna geometry depicted in Fig. 1. We see a cylindrically symmetric structure made of metal which may be excited at one or more points along its central axis by z–directed electric fields impressed between a number of gaps. The electrical properties of the material into which the antenna is radiating are assumed to be generally inhomogeneous and isotropic.

Under these conditions, the electric field will lie solely in the r–z plane and the magnetic field will only have a ϕ component. In the frequency domain (sinusoidal steady state), this situation is summarized as

$$\mathbf{E} = \Re e\left\{\boldsymbol{E}\, e^{j\omega t}\right\},$$

$$\mathbf{H} = \Re e\left\{\boldsymbol{H}\, e^{j\omega t}\right\}, \text{ where}$$

$$\boldsymbol{E} = E_r(r,z)\mathbf{a}_r + E_z(r,z)\mathbf{a}_z, \text{ and}$$

$$\boldsymbol{H} = H_\phi(r,z)\mathbf{a}_\phi.$$

The unit vectors in the r, z, and ϕ directions are $\mathbf{a}_r$, $\mathbf{a}_z$, and $\mathbf{a}_\phi$, respectively. As a consequence, Maxwell's equations take on the following form.

$$\nabla \times \boldsymbol{E} = -j\omega\mu H_\phi \mathbf{a}_\phi$$
$$= -ZH_\phi \mathbf{a}_\phi, \text{ and}$$

$$\nabla \times \boldsymbol{H} = -\frac{\partial H_\phi}{\partial z}\mathbf{a}_r + \frac{1}{r}\frac{\partial rH_\phi}{\partial r}\mathbf{a}_z$$
$$= (\sigma + j\omega\varepsilon)\boldsymbol{E} = Y^{-1}\boldsymbol{E},$$

where Z and Y are both functions of the space coordinates r and z. Eliminating $\boldsymbol{E}$ from these two expressions results in the following homogeneous equation for the distribution of magnetic field $H_\phi(r,z)$.

$$-\frac{\partial}{\partial r}\left(\frac{Y}{r}\frac{\partial rH_\phi}{\partial r}\right) - \frac{\partial}{\partial z}\left(\frac{Y}{r}\frac{\partial rH_\phi}{\partial z}\right) + \frac{Z}{r}rH_\phi = 0. \quad (1)$$

The problem is completely specified once sufficient conditions on the boundary of the domain are defined. A unique solution is obtained provided some of the boundary conditions are of the Dirichlet type with the remainder being Neumann boundary conditions.

The quantities in brackets in Eq. (1) are seen to represent the components of the

Finite Element Program

The implementation of the finite element method in FEAST is based on Burnett's UNAFEM code. The maximum number of nodes, or degrees of freedom, which FEAST can accommodate is 950, distributed over a 450 elements.

To efficiently solve complex-valued systems of linear equations of this size, FEAST employs a sparse–matrix variation of Gaussian elimination, without pivoting or scaling, which is limited to a matrix bandwidth of 100. An iterative refinement algorithm (Burden and Faires 1985, p. 438) has been incorporated into FEAST to improve the results obtained with simple Gaussian elimination.

The limits of the problem domain and the associated boundary conditions appropriate for the solution of the antenna–radiation problem given by Eqs. (3) and (5) are illustrated in Fig. 2. The Dirichlet condition $\mathcal{H}_\phi = 0$ is set on the rotational axis of symmetry, and the generalized Neumann condition, $E_{\tan(CCW)} = E_o + k\mathcal{H}_\phi$ on the remainder, where k and E_o are constants. With $k = 0$, the Neumann condition $E_{\tan(CCW)} = 0$ is applied to the horizontal symmetry plane and the antenna surfaces. Antenna excitation is specified at the feed point by defining $E_{\tan(CCW)} = E_o$ there. With $E_o = 0$ and $k = -\eta$, where η is the complex intrinsic wave impedance, the problem domain is terminated at an absorptive surface on the far boundary. This radiation or impedance boundary must be sufficiently distant from the antenna. Three wavelengths in the medium was found to be adequate when analyzing antennas with overall lengths comparable to half the wavelength in the propagation medium.

Engquist and Majda (1977) describe a highly absorbing boundary condition for use in wave-type equations. The radiation condition used in FEAST is equivalent to their first-approximation form. It is also similar to the order-1 recursion of the radiation boundary condition given by Bayliss and Turkel (1980). Engquist and Majda remark that only the first approximation condition has a physical interpretation which in our case is $\boldsymbol{E}=(\boldsymbol{H}\times\mathbf{n})/\eta$, $\mathbf{n}$ being the direction of propagation. Judging from the good agreement between the program results and the reference data as reported in the following section, a higher order absorbing boundary condition is not necessary to model the particular antenna systems that were analyzed. With $E_{\tan(CCW)} = -\eta\,\mathcal{H}_\phi$ and $\mathcal{H}_\phi$ given by ΣaN, the radiation boundary condition is implemented by transferring the additional terms in a_j from the right to the left hand side of the global system of equations.

A representative sample of the finite element mesh is also shown in Fig. 2. The actual mesh comprises 424 quadratic isoparametric triangular and quadrilateral elements which are continuous across element boundaries and are made up of 943 nodes. The nodal coordinates are normalized. In this way, antennas of varying length can be easily accommodated with the application of a geometrical scale factor. A region near the antenna is provided in which groups of nodes can be translated independently of the larger mesh to facilitate rapid modelling of a range of antenna diameters and coating thicknesses.

To model a half-wave dipole for example, the factor by which the normalized mesh would be scaled is 1λ, that is, the numerical value of one wavelength in the propa-

gation medium, expressed in meters. Using a scale factor which is near the value of one wavelength ensures that a sufficient density of nodes spans one wavelength of the electromagnetic field quantities. If the scale factor is exactly one wavelength, there will be no fewer than 10 nodes per wavelength. Modelling antennas with FEAST whose total lengths are larger than about one wavelength produces generally less accurate data because the sparsity of the nodes does not allow an accurate description of the field variations in space. Scale factors smaller than about 0.25λ, however, bring the radiation boundary too close to the antenna which may also lead to inaccurate results.

A version of FEAST has been compiled on a Macintosh II computer using Language Systems FORTRAN version 1.2.1 and the Macintosh Programmer's Workshop (MPW) version 3.0. A typical run on a 943 node system requires approximately six minutes to execute.

Validation Results

Four antenna configurations, modelled with FEAST, are considered in this paper: (1) a bare monopole over a perfectly conducting ground plane operating in air, (2) a bare center–fed dipole operating in a dissipative medium, (3) a dielectrically coated monopole in air, and (4) a dielectrically coated monopole in a lossy material. Cases (1) and (2) are examples of an antenna operating in a homogeneous medium, while cases (3) and (4) are examples of an antenna in an inhomogeneous medium. All four configurations are shown schematically in Fig. 3.

The output which FEAST generated for specific examples of these cases was compared to published data. Antenna current I was calculated from the field quantity $\mathcal{H}_\phi$ by evaluating the boundary condition for the tangential magnetic field at the surface of a perfect conductor, namely, $\mathbf{n}\times\boldsymbol{H} = \boldsymbol{J}_s$, where $\boldsymbol{J}_s$ is a surface current density. As such, $I = 2\pi\mathcal{H}_\phi$, at the antenna surface. The driving point admittance of dipoles was obtained by dividing the value of I nearest the feed point by the applied gap voltage, which is the product of gap distance and electric field. In the case of monopoles, the current and voltage were evaluated at a point on the antenna which is level with the plane of the ground. A numerical integration of the r-directed electric field estimated the voltage at that point.

Figure 4(a) shows the driving point admittance obtained with FEAST for a monopole antenna operating at 114 MHz in air for which a/λ_o is 0.0064 and b/a is 1.189 (λ_o is the free space wavelength). The data from FEAST is compared to a theoretical transmission line model published by King (1971, p. 11). For the most part, agreement is excellent. Some deviation is apparent for longer antenna lengths due to the reduction in node density which results when necessarily large scaling factors are applied to the normalized mesh. This is not a deficiency in the finite element method but a consequence of how the finite element mesh is generated in FEAST.

The data in Fig. 4(b) represents the normalized current distribution on a monopole in air with $b/\lambda_o = 0.375$, $a/\lambda_o = 0.0254$, and $b/a = 1.189$. Because the antenna length in this case permits a near optimal node density, FEAST's prediction is almost identical to the transmission–line–model theory given by King (1971, p. 17).

Driving point admittances for a dipole immersed in two different homogeneous lossy media are illustrated in Figs. 5(a) and 5(b). The frequency of operation is 114 MHz with the relative antenna radius given by $a/\lambda = 0.003175$, where λ is the wavelength in the lossy material. In one case, Fig. 5(a), the medium is characterized by an electrical conductivity of 18×10^{-3} S/m and in the other case, Fig. 5(b), by an electrical conductivity of 200×10^{-3} S/m. The same dielectric constant, $\varepsilon_r=47$, is used in both. The output from FEAST correlates quite well with the theory of Wu (1961) as presented by King (1971 p. 55). (King warns that Wu's theory is most accurate for antennas that are much longer than one wavelength.) The effect of reduced node density on calculation accuracy for antennas of longer length is apparent in Fig. 5(a). Figure 5(b), on the other hand, manifests another symptom of modelling error. In simulating a dipole antenna immersed in a homogeneous medium, FEAST includes the gap region as part of the problem domain: a gap of 0.4 mm was used in these trials. In contrast, the theoretical analysis of Wu uses a delta-function generator. As such, the losses in the gap which are modelled by FEAST tend to overestimate antenna driving point admittance, particularly for high loss media as in Fig. 5(b).

Figure 5(c) depicts the distribution of antenna current which is calculated by FEAST for a dipole operating at 114 MHz and whose dimensions are: $a/\lambda = 0.0028$, $g = 0.4$ mm, and $\beta h = 2.809$. (Here, β represents $2\pi/\lambda$, where λ is the wavelength in the lossy medium.) The lossy medium into which the antenna is propagating has an electrical conductivity of 200×10^{-3} S/m and a dielectric constant of 47. The numerical results are compared to experimental data published by King and Smith (1981, p. 166).

In testing FEAST on dielectrically coated monopoles in air, the experimental work of Lamensdorf (1967) was used as the reference. Figures 6(a) and 6(b) show the results for two antennas of identical physical dimensions, $2a = 6.35$ mm and $D = 23.77$ mm, operating at 600 MHz. In one instance, the dielectric constant of the coating is 9.0, and in the other, 15.0. Once again, the agreement is good except for longer antennas where the effects of reduced node density come into play.

The normalized antenna current distribution which corresponds to an antenna of length $h/\lambda_o = 0.5$ and for which the dielectric constant of the coating is 9.0 is illustrated in Fig. 6(c). The data of Lamensdorf (1967) and the results obtained with FEAST for magnitude and phase match reasonably well.

Limited success was realized in duplicating the experimental data of Iizuka (1963) for a dielectrically coated dipole in a lossy medium. Figure 7(a) demonstrates that, provided the antenna length is relatively small, the driving point admittance can be reliably predicted. Nothwithstanding the absolute error between Iizuka's data and the results obtained with FEAST, the general shape of the admittance profiles is replicated with only a lateral shift in the peaks. In this particular simulation, the frequency was 114 MHz with an antenna diameter $2a$ of 6.35 mm and $D/2a$ equal 1.25. The dielectric constant of the lossy medium was taken as 78 and that of the coating as 2.46. An electrical conductivity of 18×10^{-3} S/m was employed.

The normalized current distribution shown in Fig. 7(b) is for an antenna whose length βh is $\pi/2$, $2a = 6.35$ mm, and $D/2a = 4$. In this test, the conductivity of the medium was 18×10^{-3} S/m with a dielectric constant of 78, while the dielectric constant of the coating was 1.0. The imaginary part of the current is seen to be predicted quite accurately by FEAST. There is no adequate explanation for the lack of correlation exhibited by the real part of the current, however. Other sources of experimental data are being sought against which output from FEAST can be compared.

Conclusion

The generally good results demonstrated by FEAST in replicating the electrical characteristics of simple propagating wire antennas suggest that the program can model a variety of azimuthally symmetric antenna configurations. Dielectrically coated antennas operating in air or in the presence of a dissipative medium are handled equally well. FEAST is continually being validated against published antenna results and is being used to explore the characteristics of various configurations including partially coated and nonuniformly coated antennas immersed in inhomogeneous layered media.

Acknowledgments

The authors would like to thank the Alberta Oil Sands Technology and Research Authority and the Natural Sciences and Engineering Research Council of Canada for their financial support of this work.

References

Bayliss, A., and E. Turkel, "Radiation boundary conditions for wave-like equations", *Comm Pure Appl Math* **33**, 707 (1980).

Brebbia, C.A., *The Boundary Element Method for Engineers,* (Pentech Press, Plymouth, 1984).

Burden, R.L. and Faires, J.D., *Numerical Analysis,* (Prindle, Weber and Schmidt, Boston, 1985).

Burnett, D.S., *Finite Element Analysis: From Concepts to Applications,* (Addison–Wesley, Menlo Park, 1987).

Engquist, B., and A. Majda, "Absorbing boundary conditions for the numerical solution of waves", *Math Computation* **31**, 629 (1977).

Harrington, R.F., *Field Computation by Moment Methods,* (Macmillan, New York, 1968).

Hoyt, H.C., D.D. Simmonds, and W.F. Rich, "Computer designed 805 MHz proton linac cavities", *Rev Sci Instrum* **37**, 755 (1966).

Iizuka, K., "An experimental study of the insulated dipole antenna immersed in a conducting medium", *IEEE Trans Antennas Propag* **AP-11**, 518 (1963).

King, R.W.P., *Tables of Antenna Characteristics,* (IFI/Plenum, New York, 1971).

King, R.W.P., *Antennas in Matter: Fundamentals, Theory, and Applications,* (MIT Press, Cambridge, 1981).

Konrad, A., "Linear accelerator cavity field calculation by the finite element method", *IEEE Trans Nucl Sci* **NS-20**, 802 (1973).

Lamensdorf, D., "An experimental investigation of dielectric coated antennas", *IEEE Trans Antennas Propag* **AP-15**, 767 (1967).

McDonald, B.H. and A. Wexler, "Finite element solution of unbounded field problems", *IEEE Trans Microwave Theory Tech* **MTT-20**, 841 (1972).

McDougall, M.J. and J.P. Webb, "Infinite elements for the analysis of open dielectric waveguides", *IEEE Trans Microwave Theory Tech* **MTT-37**, 1724 (1989).

Morgan, M.A., S-K. Chang, and K.K. Mei, "Coupled azimuthal potentials for electromagnetic field problems in inhomogeneous axially symmetric media", *IEEE Trans Antennas Propag* **AP-25**, 413 (1977).

Paulsen, K.D., D.R. Lynch, and J.W. Strohbehn, "Three-dimensional finite, boundary, and hybrid element solutions of the Maxwell equations for lossy dielectric media", *IEEE Trans Microwave Theory Tech* **MTT-36**, 682 (1988).

Wu, T.T., "Theory of the dipole antenna and the two-wire transmission line", *J Math Phys* **2**, 550 (1961).

Zienkiewicz, O.C., *The Finite Element Method,* (McGraw–Hill, London, 1985).

Figure 1

General, cylindrically symmetric antenna structure and coordinate system.

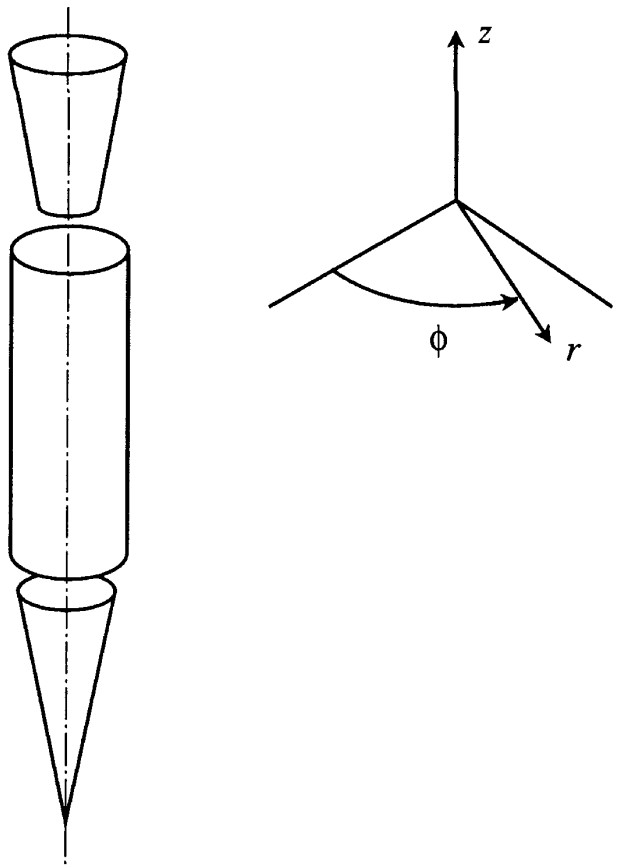

Figure 2

Outline of the normalized finite element mesh used by FEAST to simulate metal-wire dipole and monopole antennas. The appropriate boundary conditions are also shown.

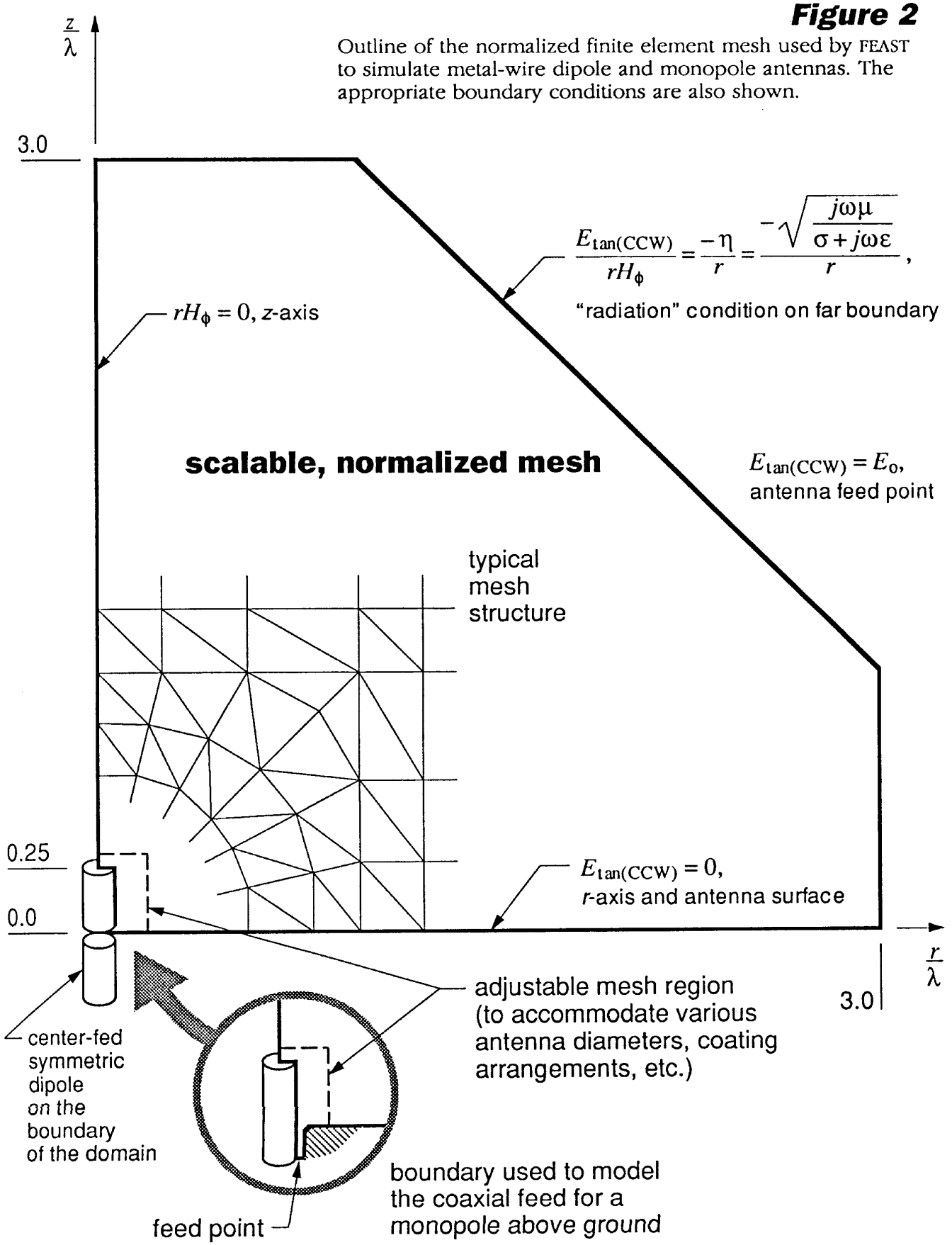

Figure 3

The four antenna configurations which were modelled with FEAST for the purpose of validation.

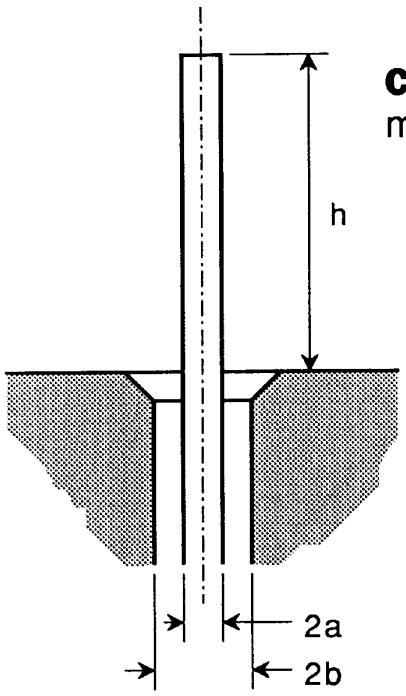

Case 1
monopole in air

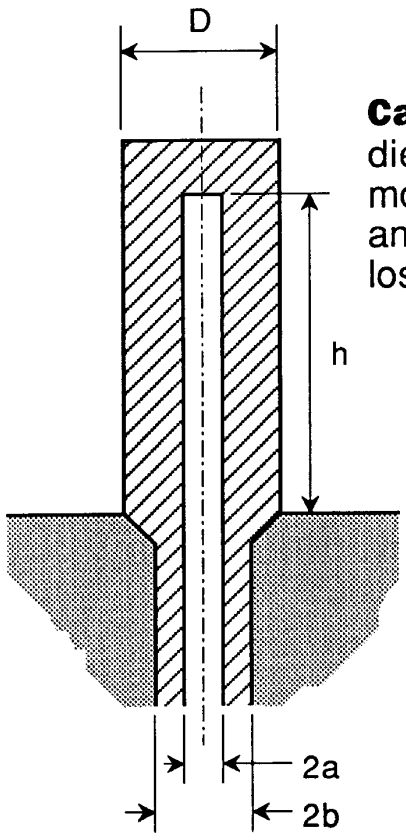

Case 3 & 4
dielectric-coated monopole in air and a lossy material

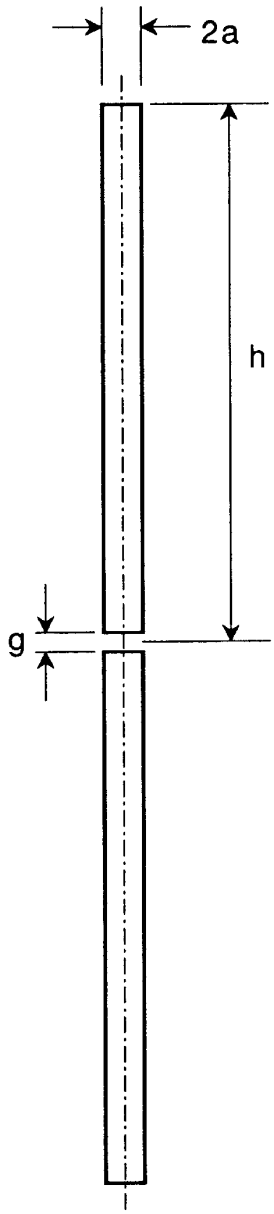

Case 2
dipole in a lossy material

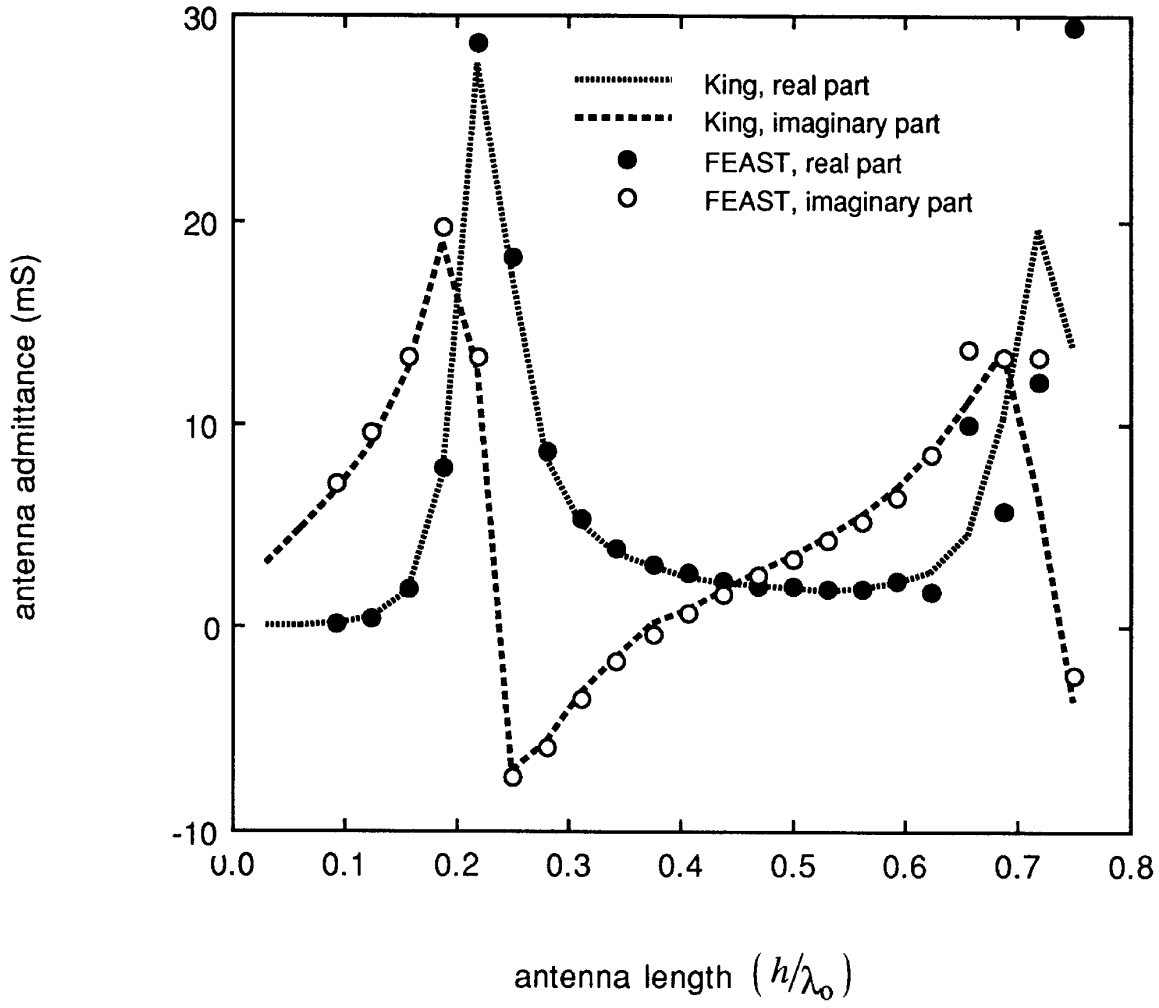

Figure 4(a) Antenna driving point admittance versus antenna length for a bare monopole over a conductive plane radiating into air. FEAST output is compared to theoretical data published by King (1971, p. 11).

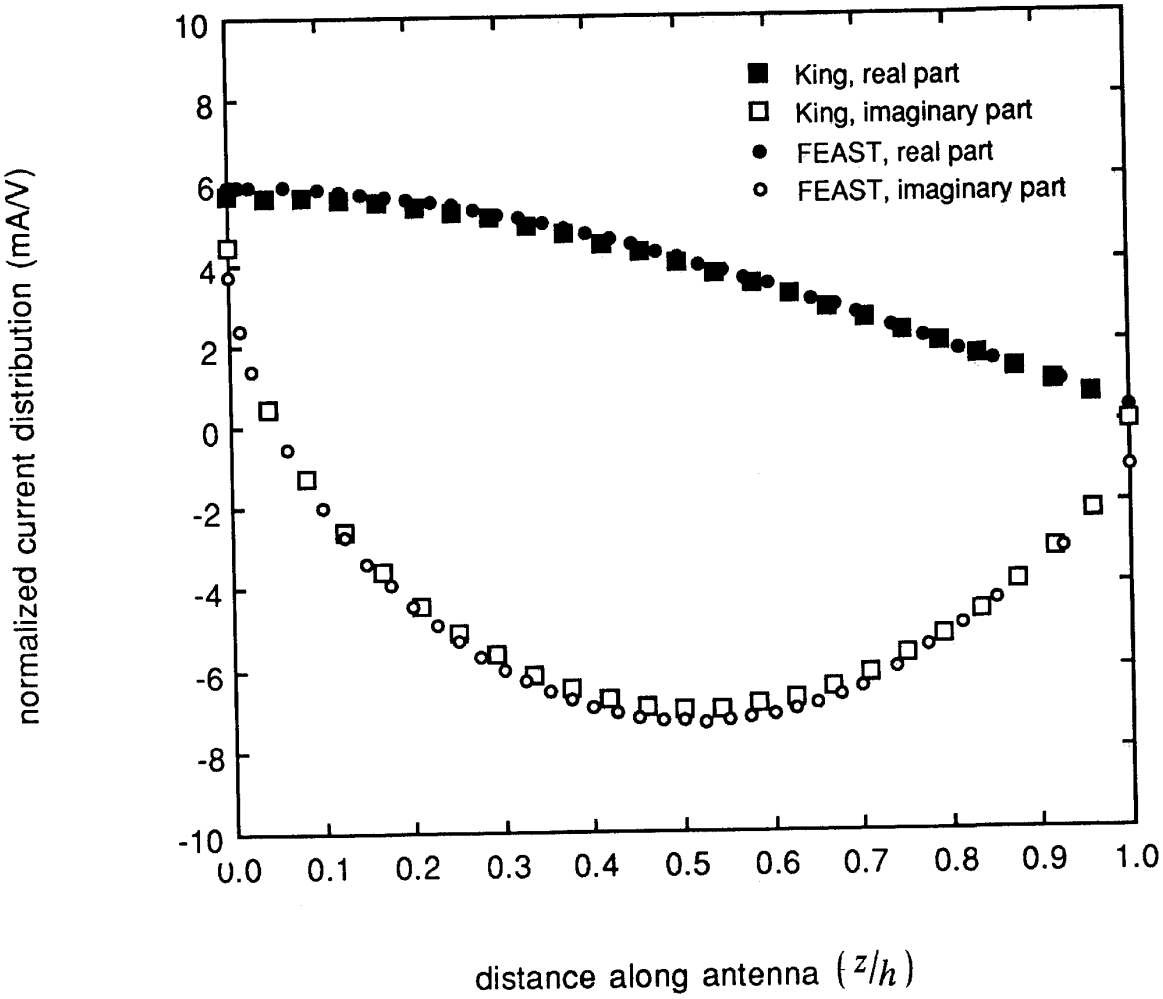

monopole in air

frequency = 114 MHz
h/λ_o = 0.375
a/λ_o = 0.0254
b/a = 1.189

Figure 4(b) Normalized antenna current distribution for a bare monopole over a conductive plane radiating into air. FEAST output is compared to theoretical data published by King (1971, p. 17).

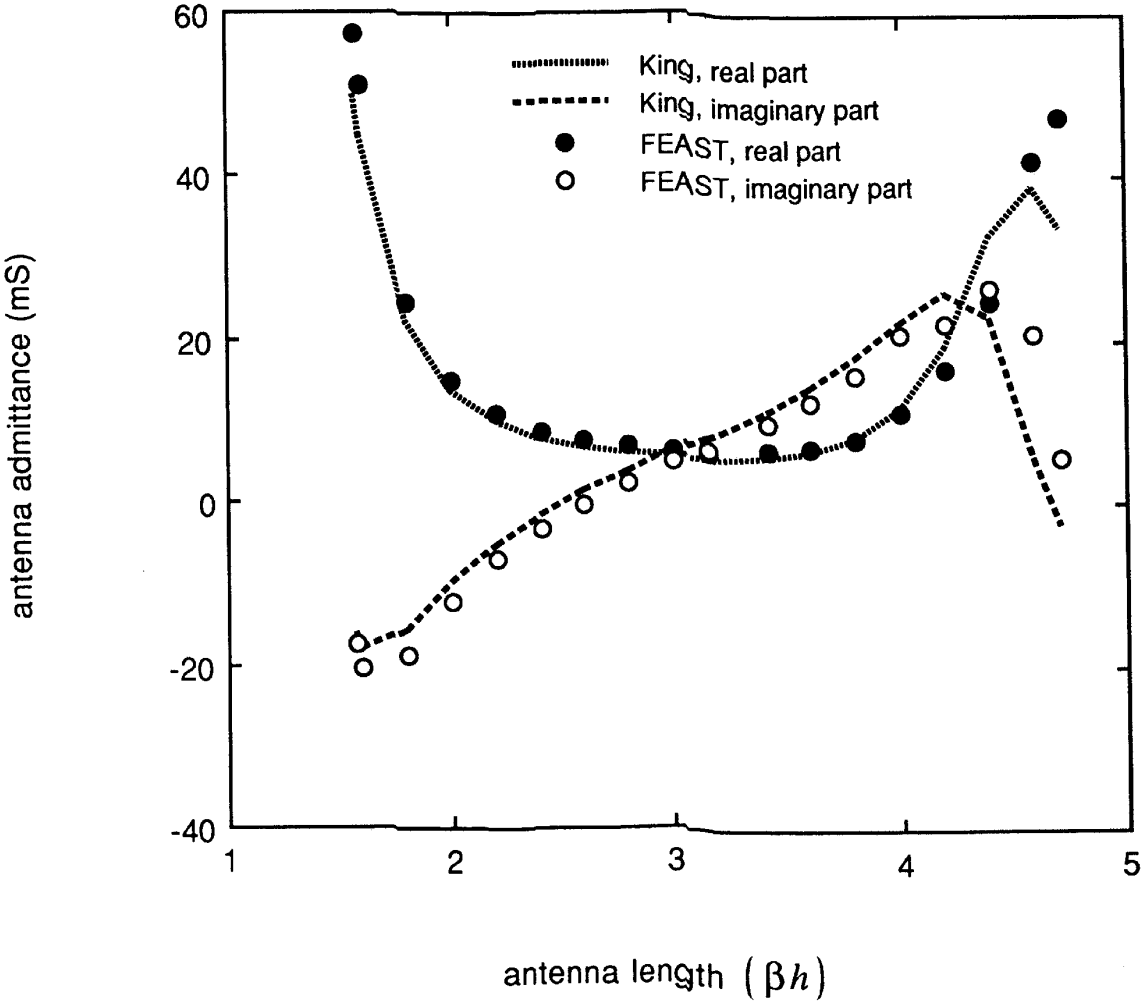

dipole in lossy medium

frequency = 114 MHz
a/λ = 0.003175
g = 0.0004 m
σ = 18 mS/m
ε_r = 47

Figure 5(a) Comparison between the antenna admittance versus antenna length predicted by FEAST and the theoretical values given by King (1971, p. 55) for a dipole antenna operating in a dissipative medium.

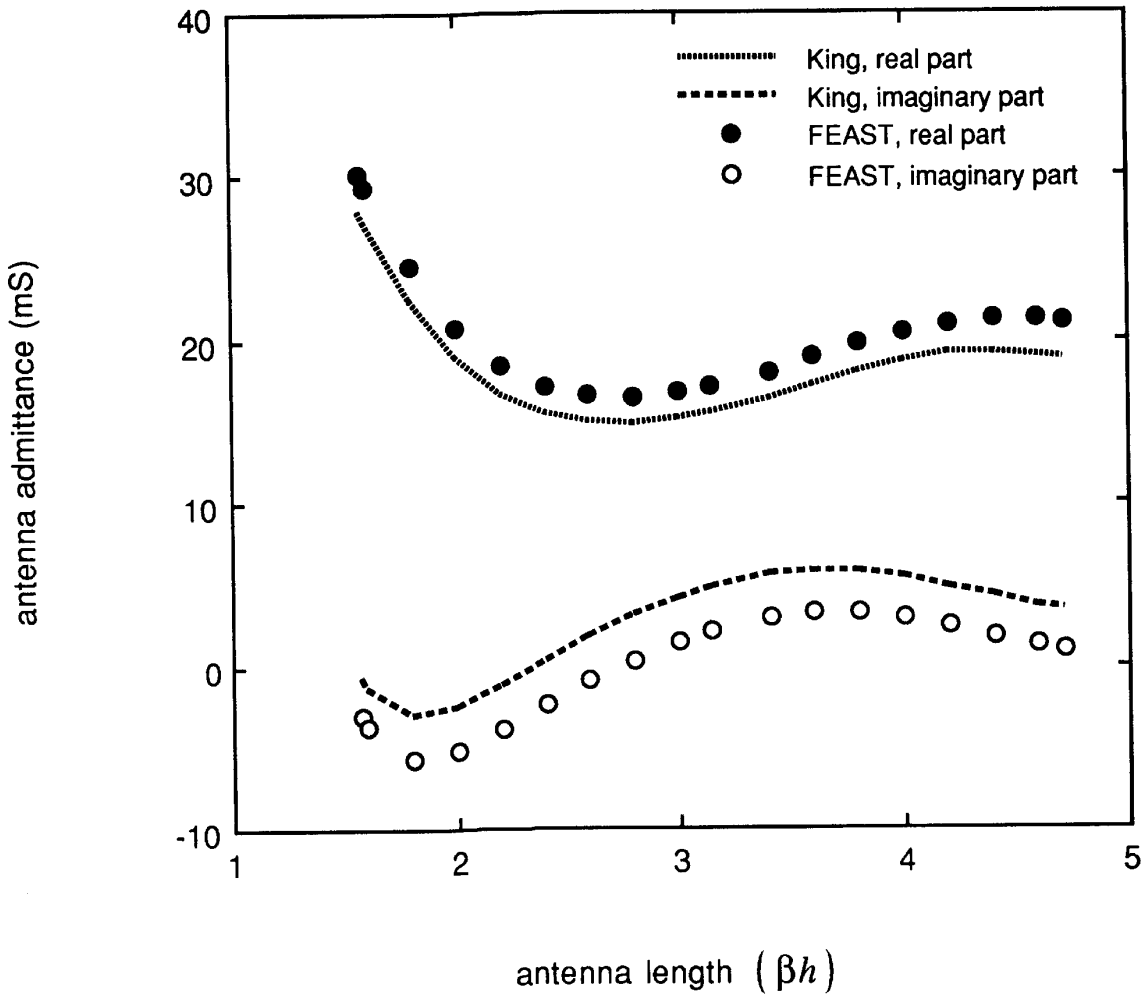

dipole in lossy medium

frequency = 114 MHz
a/λ = 0.003175
g = 0.0004 m
σ = 200 mS/m
ε_r = 47

Figure 5(b) Comparison between the antenna admittance versus antenna length predicted by FEAST and the theoretical values given by King (1971, p. 55) for a dipole antenna operating in a dissipative medium.

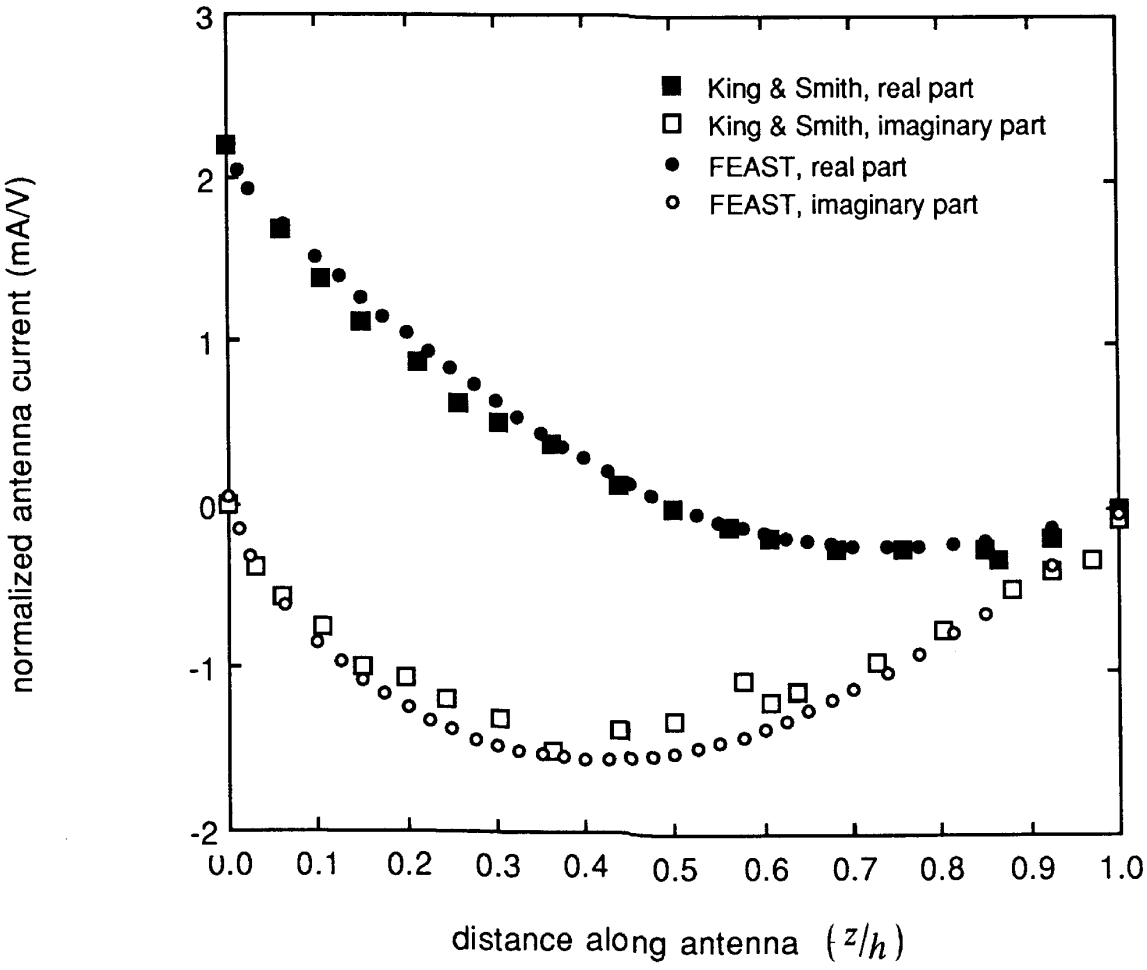

dipole in lossy medium

frequency = 114 MHz
a/λ = 0.0028
g = 0.0004 m
σ = 200 mS/m
ε_r = 47
βh = 2.809

Figure 5(c) Normalized antenna current distribution curves are shown for the case of a dipole immersed in a dissipative medium. An experimental curve extracted from King and Smith (1981, p. 166) is given as well as data calculated with FEAST.

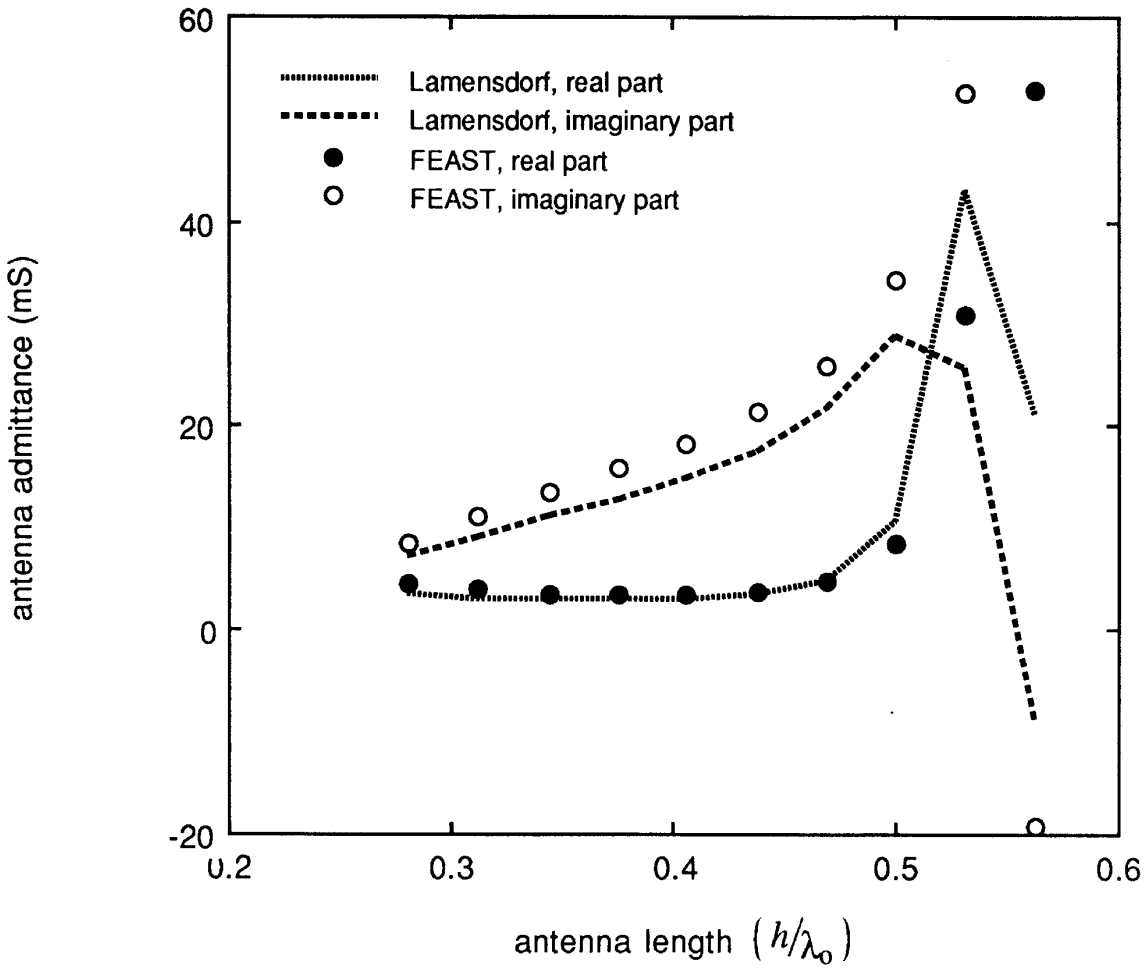

dielectrically coated monopole in air

frequency= 600 MHz
$2a$ = 0.25 in. (6.35 mm)
D = 0.936 in. (23.77 mm)
ε_r = 9

Figure 6(a) Experimental data collected by Lamensdorf (1967) for the driving point admittance versus antenna length of a dielectrically coated monopole operating in air is compared to the FEAST simulation of the same antenna.

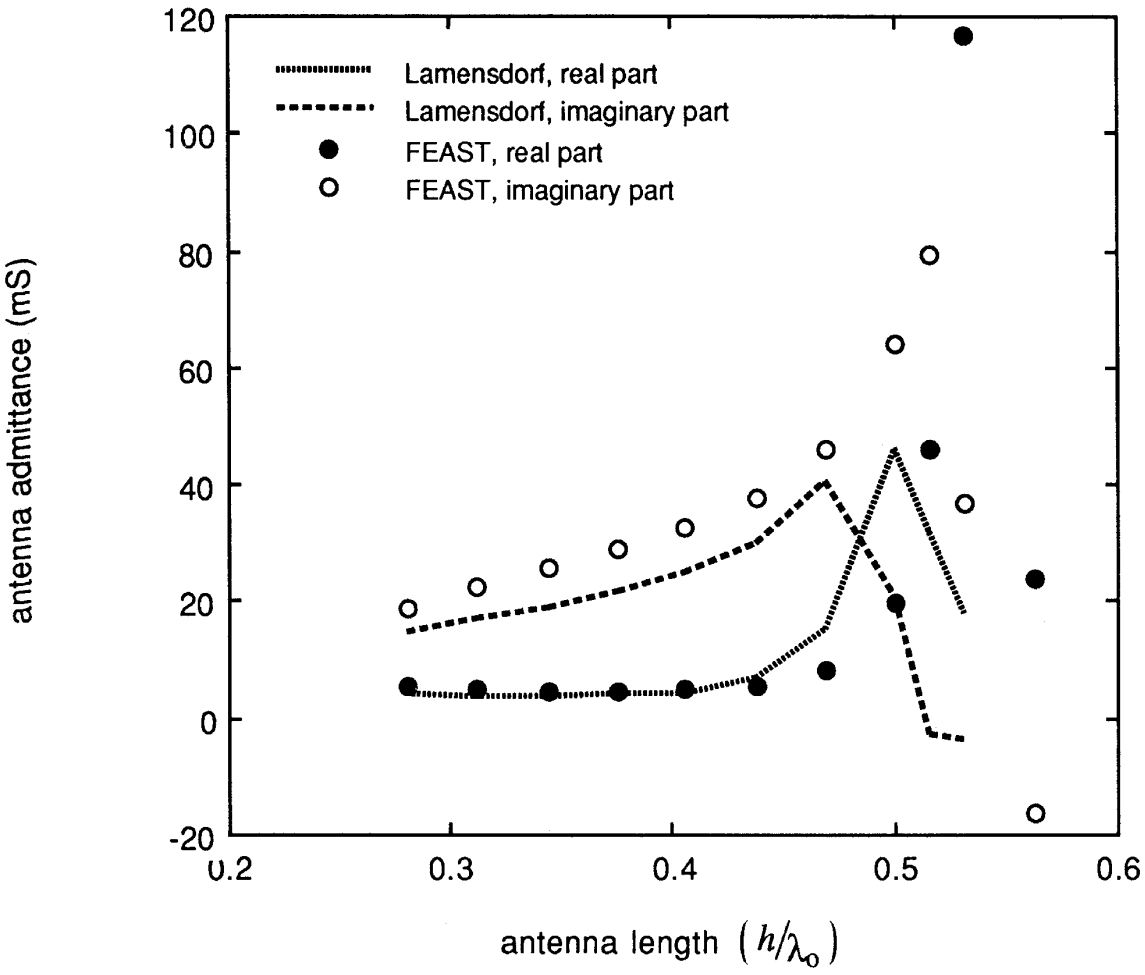

dielectrically coated monopole in air

frequency= 600 MHz
$2a$ = 0.25 in. (6.35 mm)
D = 0.936 in. (23.77 mm)
ε_r = 15

Figure 6(b) Experimental data collected by Lamensdorf (1967) for the driving point admittance versus antenna length of a dielectrically coated monopole operating in air is compared to the FEAST simulation of the same antenna.

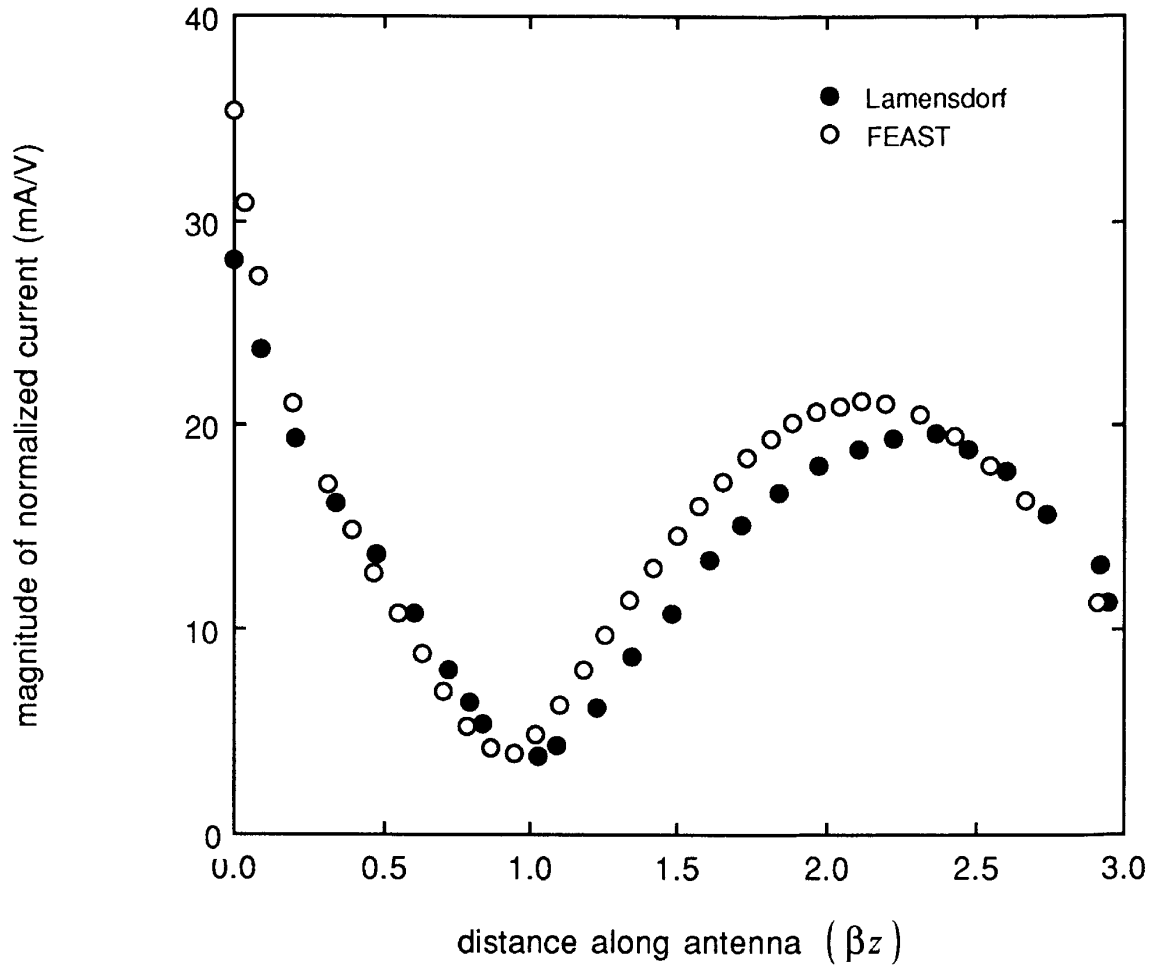

dielectrically coated monopole in air

frequency= 600 MHz
h/λ_o = 0.5
$2a$ = 0.25 in. (6.35 mm)
D = 0.936 in. (23.77 mm)
ε_r = 9

Figure 6(c) Magnitude of the normalized current distribution on a dielectrically coated monopole in air. Output from FEAST is compared to the experimental data of Lamensdorf (1967).

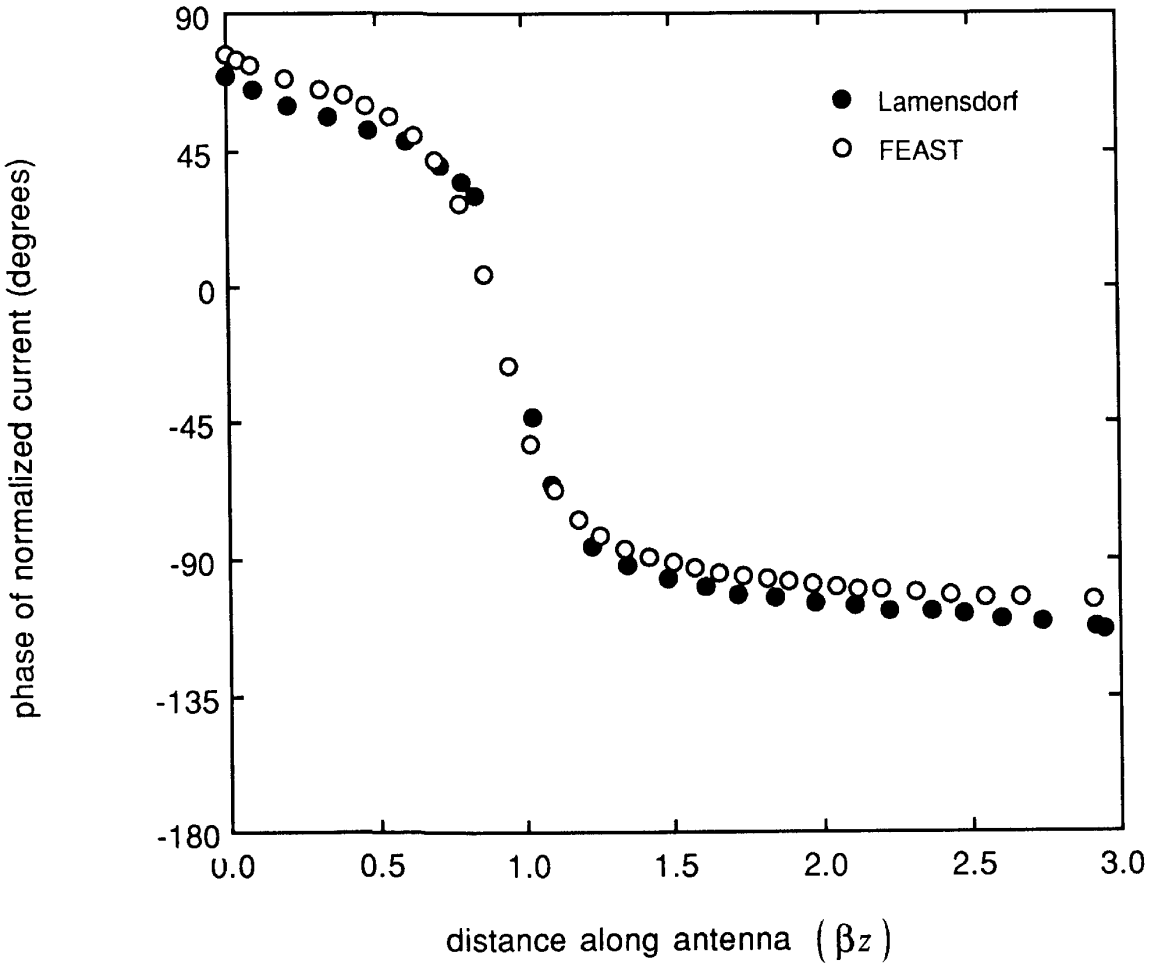

dielectrically coated monopole in air

frequency= 600 MHz
h/λ_o = 0.5
$2a$ = 0.25 in. (6.35 mm)
D = 0.936 in. (23.77 mm)
ε_r = 9

Figure 6(c) (continued) Phase of the normalized current distribution on a dielectrically coated monopole in air. Output from FEAST is compared to the experimental data of Lamensdorf (1967).

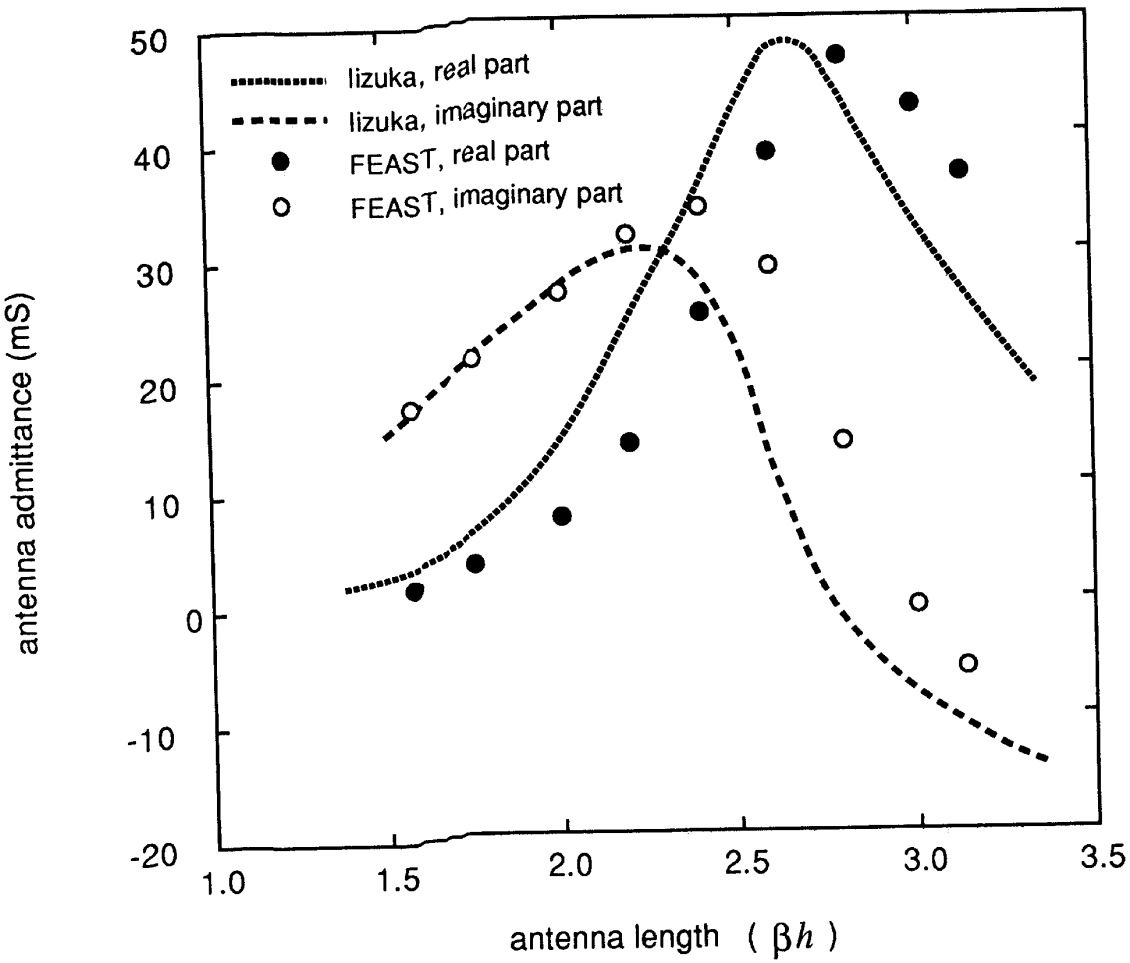

dielectrically coated dipole in a lossy medium

frequency= 114 MHz
$2a$ = 0.25 in. (6.35 mm)
$D/2a$ = 1.25
ε_r = 78 (medium)
ε_r = 2.46 (coating)
σ = 18 mS/m

Figure 7(a) Driving point admittances of dielectrically coated dipoles of varying length immersed in a lossy medium. Results predicted by FEAST are compared to the measured values of Iizuka (1963).

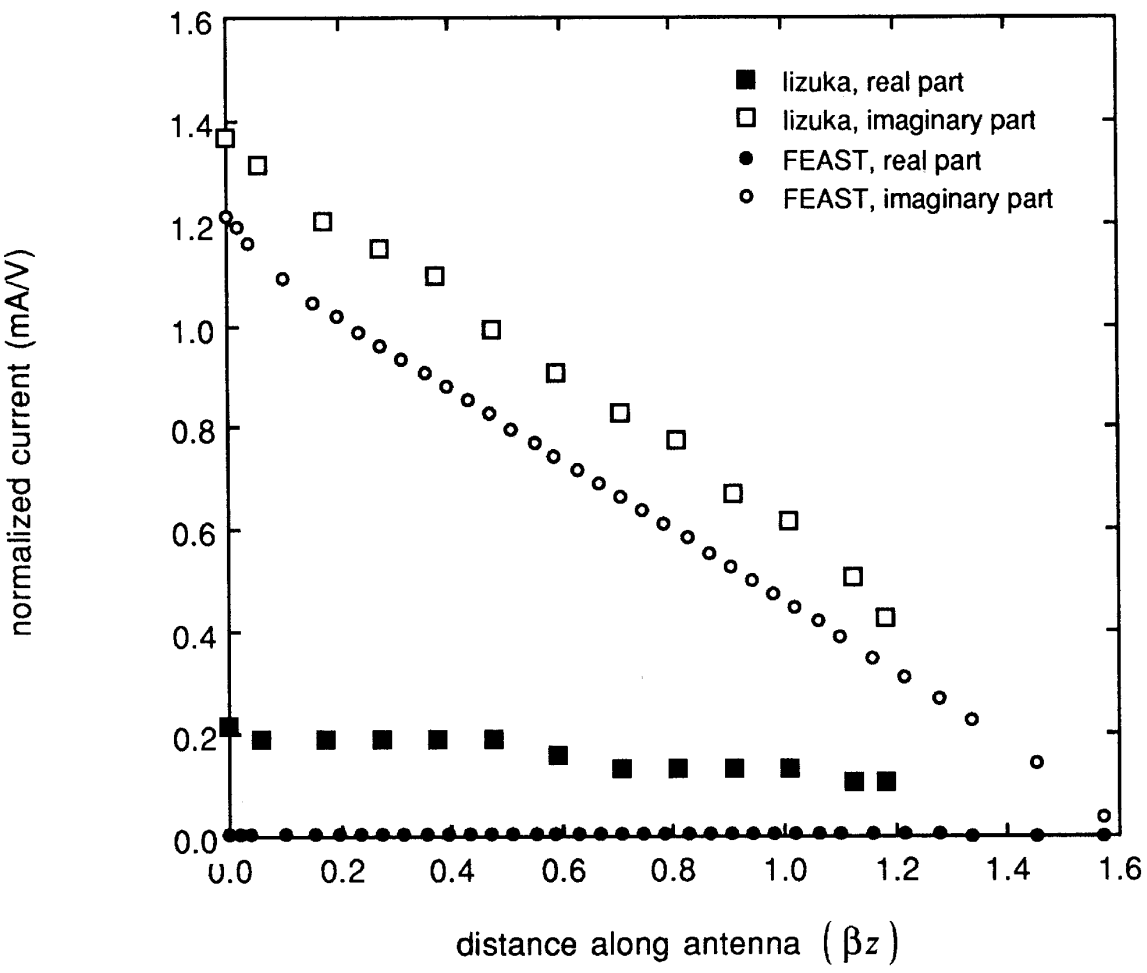

dielectrically coated dipole in a lossy medium

frequency= 114 MHz
$\beta h = \pi/2$
$2a$ = 0.25 in. (6.35 mm)
$D/2a = 4$
$\varepsilon_r = 78$ (medium)
$\varepsilon_r = 1.0$ (coating)
σ = 18 mS/m

Figure 7(b) Current distribution along a dielectrically coated dipole immersed in a lossy medium as predicted by FEAST and as measured by Iizuka (1963).